Split-Cylinder Resonant Electron Polarimeter

Richard Talman
Laboratory for Elementary-Particle Physics
Cornell University

June, 2017

Abstract

Recent proposals to measure the proton electric dipole moment (EDM) use protons circulating in a storage ring with their spins "frozen" parallel or anti-parallel to their velocities. Polarimetry is required both to stabilize the frozen spin operation and to measure the EDM-induced precession. This paper proposes a test of resonant electron (rather than proton) polarimetry using a polarized 0.5 MeV kinetic energy, 500 MHz bunch frequency linac electron beam at Jefferson Laboratory. The resonator is a 5 cm long copper cylinder, sliced longitudinally by a single 1 mm gap that serves as the capacity C of a high frequency LC or microwave oscillator; the inductance L is provided by the conducting cylinder serving as a single turn solenoid. As a longitudinally polarized electron bunch passes through the resonator its magnetization excites the fundamental oscillation mode of the resonator. The polarimeter detects and measures the longitudinal component of polarization by a kind of inverse NMR in which the nuclear magnetic moments excite an external cavity, rather than the other way round. Successive bunches are arranged to have alternating forward and backward polarizations. This moves the beam polarization frequency to odd harmonics of 250 MHz, away from the direct beam charge frequency harmonics. This greatly suppresses the "background" response to be beam charge relative to the "foreground" polarization response.

Contents

1 Introduction

A proposed experiment to measure the proton electric dipole moment (EDM) uses protons stored in a fully-electrostatic storage ring. The main bending field is produced by applying a voltage between inner and outer chamber walls. The full ring consists of repetitions of these sector bends separated by drifts, quadrupoles, RF cavities and so on. The nominal design orbit consists of circular arcs of radius r_0 joined by straight lines through straight sections.

To reduce systematic errors there will be two counter-circulating polarized beams, as nearly identical as possible. The polarizations of both beams will be "frozen", parallel or anti-parallel to the beam directions. Polarimetry (i.e. measuring the polarization of each circulating bunch) is required to monitor and stabilize this frozen spin operation.

Acting on whatever EDM the protons possess, the (dominant) radial electric field tends to tip the beam polarizations up or down. It is this tipping that is to be measured to obtain the proton EDM. Ability to perform this measurement sets stringent polarimetry requirements.

This paper proposes a test of resonant electron (rather than proton) polarimetry using a polarized 0.5 MeV kinetic energy, 500 MHz bunch frequency linac electron beam at Jefferson Laboratory.

2 Resonant polarimetry

2.1 Apparatus

Consider a single, longitudinally polarized bunch of electrons in a linac beam that passes through the split-cylinder resonator shown in Figure 1. The split cylinder can be regarded as a one turn solenoid.

The bunch polarizations will toggle, bunch-to-bunch, between directly forward and directly backward. This is achieved by having two symmetrically interleaved beams, an A beam and a B beam, each having bunch repetition frequency $f_0 = 0.25\,\mathrm{GHz}$ (4 ns bunch separation). The resonator harmonic number, relative to f_0 is an odd number, tentatively it is $h_c = 11$. Irrespective of polarization, the charged bunch frequency will be $2f_0 = 0.5\,\mathrm{GHz}$. Treated as an LC circuit, the split cylinder inductance is L_c and the gap capacity is C_c. In practice the bunches will be only partially polarized but, for estimating the signal strength and signal to noise ratio we assume the bunches are 100%, longitudinally polarized.

2.2 Resonator parameters

The highly conductive split-cylinder can be treated as a one-turn solenoid. In terms of its current I, its magnetic field B is given by

$$B = \mu_0 \frac{I}{l_c}, \tag{1}$$

and its magnetic energy W_m can be expressed either in terms of B or I;

$$W_m = \frac{1}{2}\frac{B^2}{\mu_0}\pi r_c^2 l_c = \frac{1}{2} L_c I^2. \tag{2}$$

Its self-inductance is therefore

$$L_c = \mu_0 \frac{\pi r_c^2}{l_c}. \tag{3}$$

The gap capacitance (with gap g_c reckoned for vacuum dielectric and fringing neglected) is

$$C_c = \epsilon_0 \frac{w_c l_c}{g_c}. \tag{4}$$

Other resonator parameters, with proposed values, are given in Table 1.

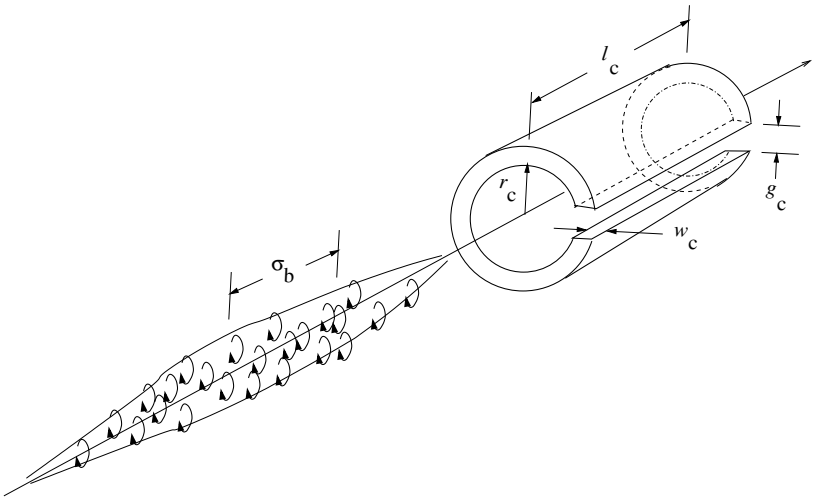

Figure 1: Perspective view of polarized beam bunch passing through the polarimeter. Dimensions are shown for the polarized proton bunch and the split-cylinder copper resonator, and listed in Table 1. For the proposed test using a polarized electron beam at Jefferson Lab, the bunch will actually be somewhat shorter than the cylinder, and have a beer can shape.

3 "Local" Lenz law (LLL) approximation

A "local" Lenz law approximation for calculating the current induced in our split cylinder by a passing polarized beam bunch is introduced by Figure 3. The split cylinder resonator is treated as a one turn solenoid and, for simplicity, the electron bunch is assumed to have a beer can shape, with length l_b and radius r_b. The magnetization $\mathbf{M}$ within length Δz of a beam bunch (due to all electron spins in the bunch pointing, say, forward) is ascribed to azimuthal Ampẽrian current $\Delta I_b = i_b \Delta z$. In other words, in the volume within the beam bunch the magnetic field is also a perfect solenoid (with end fields being neglected).

For sufficiently short cylinder lengths, the bunch transit time will be short compared to the oscillation period of the split cylinder and the presence of the gap in the cylinder produces negligible suppression of the Lenz's law current induced by the passing bunch (because the charge piles up harmlessly on the capacitance of the gap). Define i_{LL} to be the Lenz law current per longitudinal length. Then $\Delta I_{LL} = i_{LL}\Delta z$ is the induced azimuthal current shown in the (inner skin depth) of the cylinder, in the "local region" of the figure. To prevent any net flux from being present locally within the section of length Δz, the flux due to the induced Lens law current must cancel the Ampère flux.

The Lenz law magnetic field is $B_{LL} = \mu_0 i_{LL}$ and the magnet flux through the cylinder is

$$\phi_{LL} = \mu_0 \pi r_c^2 i_{LL}. \tag{5}$$

According to Jackson's[2] section 5.10, the magnetic field $\mathbf{B_b}$ within the polarized beam bunch is equal to $\mu_0 \mathbf{M_b}$ which is the magnetization (magnetic moment per unit volume) due to the polarized electrons.

$$B_b = \mu_0 M_B = \mu_0 \frac{N_e \mu_B}{\pi r_b^2 l_b}, \tag{6}$$

where N_e is the total number of electrons in each bunch. The flux through Δz due to this interval

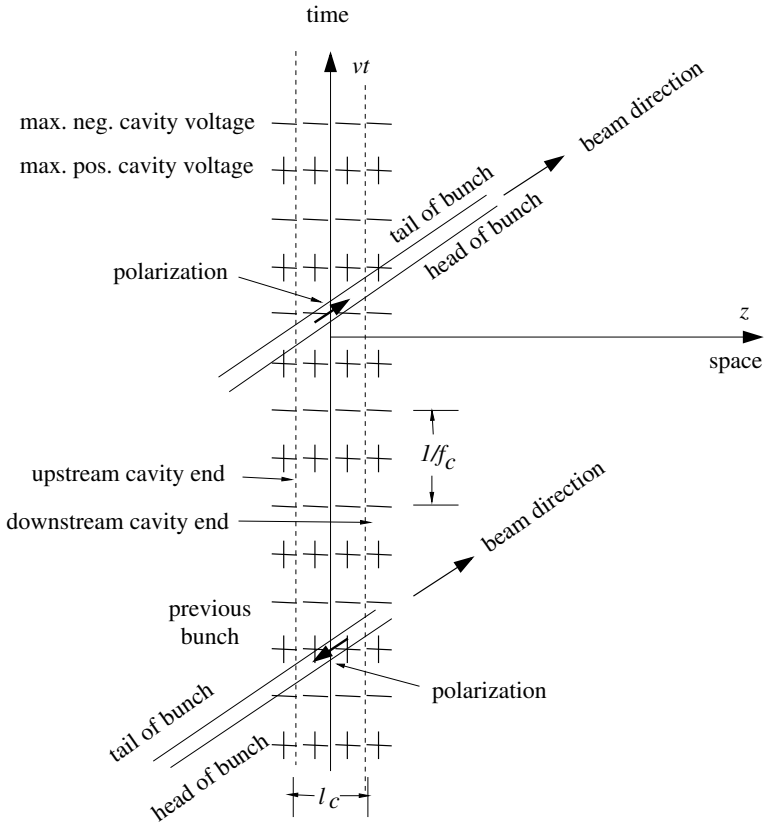

Figure 2: Space-time plot showing entry of the front, followed by exit from the back of one bunch, followed by the entrance and exit of the following bunch. Bunch separations and cavity length are arranged so that cavity excitations from all four beam magnetization exitations are perfectly constructive, but direct excitation by bunch charge is perfectly destructive. The rows ++++ and ---- represent equal time contours of maximum or minimum V_C, E_ϕ, dB_z/dt, or dI_C/dt, all of which are in phase. (Unlike all other figures and examples, which use $h_c = 11$) for this figure the harmonic number is $h_c = 7$.

of the beam bunch is therefore

$$\phi_b = B_b \pi r_b^2 = \mu_0 \frac{N_e \mu_B}{l_b}. \tag{7}$$

Since the Lenz law and bunch fluxes have to cancel we obtain

$$i_{LL} = -\frac{N_e \mu_B}{l_b} \frac{1}{\pi r_c^2}. \tag{8}$$

For a bunch that is longitudinally uniform (as we are assuming) we can simply take $\Delta z = l_b$ and obtain

$$I_{LL} = i_{LL} l_b = -\frac{N_e \mu_B}{\pi r_c^2} \frac{\Delta z}{l_b}. \tag{9}$$

Once the bunch is fully within the cylinder, I_{LL} "saturates", no longer increasing proportional to Δz.

We now make the further assumption (somewhat contradicting the figure, but consistent with the proposed J-LAB test) that the bunch is sufficiently shorter than the cylinder (i.e. $l_b << l_c$)

parameter name	parameter symbol	formula	unit	value
cylinder length	l_c		m	0.04733
cylinder radius	r_c		m	0.01
gap height	g_c		m	0.00103943
wall thickness	w_c		m	0.001
capacity*	C_c	$\epsilon_0 \frac{w_c l_c}{g_c/\epsilon_r}$	pF	0.40317
inductance	L_c	$\mu_0 \frac{\pi r_c^2}{l_c}$	nH	8.3411
resonant freq.	f_c	$1/(2\pi\sqrt{L_c C_c})$	GHz	2.7445
resonator wavelength	λ_c	c/f_c	m	0.10923
copper resistivity	$\rho_{\rm Cu}$		ohm-m	1.68e-8
skin depth	δ_s	$\sqrt{\rho_{\rm Cu}/(\pi f_c \mu_0)}$	μm	1.2452
eff. resist.	R_c	$2\pi r_c \rho_{\rm Cu}/(\delta_s l_c)$	ohm	0.017911
quality factor	Q_c			8030.7
resonant factor	Q_c/h_c			
bunch frequency	$f_A = f_B = f_0$		GHz	0.2495
cavity harm. number	h_c	f_c/f_0		11
electron velocity	v_e	$c\sqrt{1-1/2^2}$	m/s	2.5981e8
cavity transit time	Δt	l_c/v_e	ns	0.18230
transit phase advance	$2\pi f_0 \Delta t$	$2\pi f_0 l_c/v_e$		0.28578
transit cycle advance	$\Delta\phi_c$	$f_c \Delta t$		0.50032
electrons per bunch	N_e			2×10^6
bunch length	l_b		m	0.01
bunch radius	r_b		m	0.005
entry cycle advance		$\Delta\phi_c l_b/l_c$		0.15011

Table 1: Resonator and beam parameters. The capacity has been calculated using the parallel plate formula. The true capacity will probably be somewhat greater, and the the gap g_c will have to be adjusted to tune the natural frequency. When the A and B beam bunches are symmetrically interleaved, the bunch repetition frequency (with polarization ignored) is $2f_0$.

that the linear build up of I_{LL} can be ascribed to the constant applied voltage V_{LL} required to satisfy Faraday's law.

For a CEBAF I_e =160 μA, 0.5 GHz bunch frequency beam the number of electrons per bunch is approximately 2×10^6. Using parameters from Table 1 we obtain the saturation level Lenz law current to be

$$I_{LL}^{\rm sat.} = -\frac{N_e \mu_B}{\pi r_c^2} \quad \Big(\stackrel{\rm e.g.}{=} -5.9078 \times 10^{-14}\,{\rm A} \Big). \tag{10}$$

The charge that has flowed onto the capacitor during the linear current entrance build up, at the instant the bunch is fully within the cylinder is

$$Q_1^{\rm max.} = \frac{1}{2}\, I_{LL}^{\rm sat.} \frac{l_b}{v_e} \quad \Big(\stackrel{\rm e.g.}{=} -1.6156 \times 10^{-24}\,{\rm C.} \Big). \tag{11}$$

The meaning of the superscript "max" is that, if there were no further resonator excitations, the charge on the capacitor would oscillate between $-Q_1^{\rm max.}$ and $Q_1^{\rm max.}$. All that remains to do is to confirm the perfectly-constructive, coherent build-up indicated in Figure 2, and to calculate the factor by which this maximum capacitor has increased when the steady-state corcuit response has been reached.

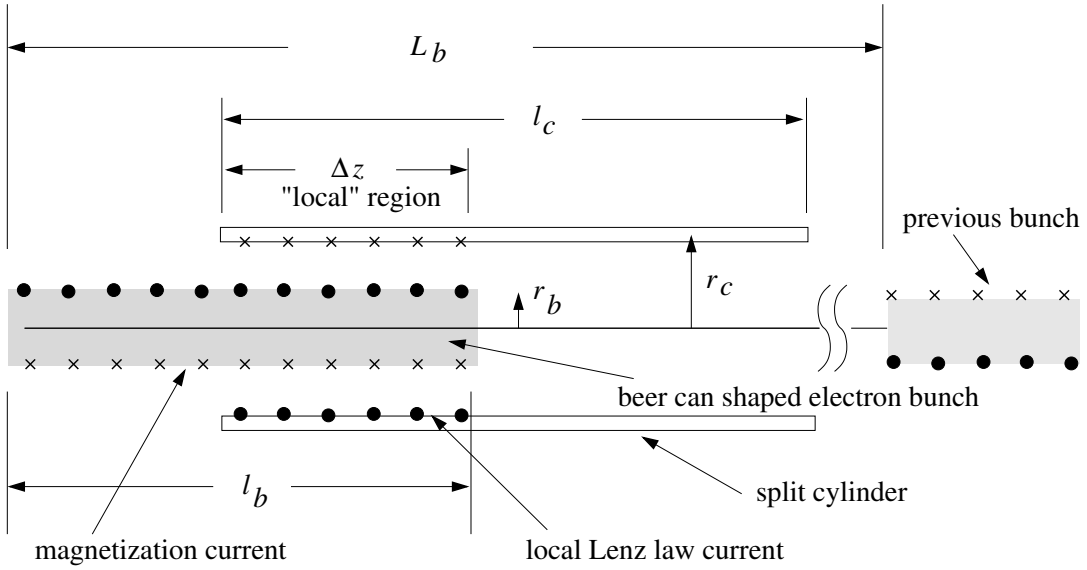

Figure 3: Schematic of beer-can-shaped electron bunch entering the split-cylinder resonator, which is longer than the bunch. Lenz's law is applied to the local overlap region of length Δz. Flux due to the induced Lenz law current is assumed to exactly cancel locally the flux due to the Ampère bunch polarization current.

For comparison of different signal levels in a consistent way in this paper, the energy transferred to the capacitor during a single bunch passage will be be adopted. For the foreground, beam magnetization signal just analysed, this quantity will be designated $U_1^{\text{pol.}}$. This is the "foreground" quantity that, magnified by a resonant amplitude magnification factor M_r^2 will provide the actual polarization measure in the form of steady-state energy $U^{\text{pol.}}$ stored on the capacitor;

$$\boxed{U^{\text{pol.}} = \frac{1}{2}\,\frac{Q_1^{\text{max.}\,2}}{C_c}\,M_r^2\cos\psi = \left(3.2\times10^{-36}\,\text{J}\right)M_r^2\cos\psi} \tag{12}$$

where, as calculated in Eq. (11), $Q_1^{\text{max.}} = 1.62\times10^{-24}\,\text{C}$ is the charge deposited on the resonator capacitance during a single bunch passage of a bunch with the nominal ($N_e = 2\times10^6$ electrons) charge. The final $\cos\psi$ factor is an arbitrary phase factor that will be explained later, in connection with synchronous detection. This equation is boxed to emphasize the importance of $U_1^{\text{pol.}}$ in absolute terms, but also for relative comparison with "background" other excitation sources which deposit spurious capacitor energy changes and which will also be boxed.

Except for the back voltage due to charge accumulating on the capacitor, $I_{LL}^{\text{sat.}}$ is the constant current that would flow in the inductance while the first bunch remains within the cylinder. But, because the resonator natural frequency is so high, it is not legitimate to neglect the back voltage. As Figure 2 indicates, by the time the bunch exits the cylinder, the capacitor voltage is supposed to be just reversed. The transit time is

$$\Delta t = \frac{l_c}{v_e} \quad \overset{\text{e.g.}}{=} \quad \frac{0.04733}{2.598\times10^8} = 0.1825\,\text{ns}, \tag{13}$$

for which, $f_c\Delta t = 0.5$. As a result the (now negative) Lenz e.m.f. during the exit effectively doubles the amount of charge that, in effect, has been allowed to bypass the inductance, to appear on the capacitor.

In a lumped constant circuit model $Q^{\max.} = 2Q_1^{LL}$ is the excess (maximum) charge on the capacitor due to the passage of the first bunch. Without subsequent bunch passages this maximum charge would decay exponentially with time constant $\tau_c = 2Q/\omega_0$, where Q is the resonator "quality factor".

As Figure 2 also indicates, the parameters have been adjusted so that all bunch entrances and exits contribute constructively to $Q^{\max.}$. On subsequent bunch passages there will already be current flowing due to previous bunch passages. Eventually a steady state will be achieved, in which the resonator energy gained during each bunch passage exactly cancels the ohmic energy lost during the interval between bunch passages.

4 Resonant excitation

When a longitudinally polarized bunch enters the conducting cylinder its magnetization tries to change the flux linking the cylinder. By Lenz's law this change in flux is opposed by azimuthal current flowing in the cylinder. The resulting voltage due to charge on the capacitor opposes and, after many cycles, establishes a steady state in which the induced response each cycle just matches the resistive decay of the resonator.

In any case the Lenz law current is present only while the bunch is passing through the cylinder. It is a quite good approximation to treat the applied voltage as having a square "top hat" shape, with one sign on entry and the opposite sign on exit. For the circuit to respond to beam magnetization, but not to the charge itself, the bunch magnetizations alternate, pulse-to-pulse. This is accomplished by tuning the resonator to an odd harmonic of the bunch frequency divided by 2.

The effect of the pulse-to-pulse toggling of the polarization is the reduce the (current-weighted) polarization frequency from 0.5 GHz to 0.25 GHz. Odd harmonics of 0.25 GHz that are excited by the beam polarization will therefore be isolated in the frequency domain by direct current excitation at harmonics of 0.5 GHz.

In actual practice, as well as having alternating polarization, the bunch charge will also have slightly different charges, which will cause some direct current excitation to leak into odd harmonics. However this spurious signal will also be reduced by the symmetry of the split-cylinder configuration. Even for imperfect alignment and positioning the direct charge excitation will therefore be further reduced.

In a MAPLE program used to calculate the response, the excitation is modeled using "piecewise defined" train of pulses. The bipolar pulses modeling entry to and exit from the resonator are obtained as the difference between two "top hat" pulse trains, one slightly displaced from the other in time. Here is a fragment of this code:

```
TopHatAltWave0p3 := t-> piecewise(
                        0<(t-0.3) and t<  0+(1+0.3),  1,
                       11<(t-0.3) and t< 11+(1+0.3), -1,
                       22<(t-0.3) and t< 22+(1+0.3),  1,
                       33<(t-0.3) and t< 33+(1+0.3), -1,
                          ..................
                      572<(t-0.3) and t<572+(1+0.3),  1,
                      583<(t-0.3) and t<583+(1+0.3), -1,
                      594<(t-0.3) and t<594+(1+0.3),  1,
                      605<(t-0.3) and t<605+(1+0.3), -1,
                      616<(t-0.3) and t<616+(1+0.3),  1, 0):

                          ..................
```

```
TopHatAltWaveDiff := t-> TopHatAltWave0(t) - TopHatAltWave0p3(t):
```

The last line shows the subtraction of a wave displaced by 0.3 time units (the earlier instructions show a few lines) from an identical, but undisplaced train.

In this form the bipolar pulse separations are 1 unit and the bunch-to-bunch separations are 11 units. (The choice of 11 is based on the tentatively adopted harmonic number $h_c = 11$, which is the ratio between resonator frequency and (same polarity) bunch frequency.) Two short sections of the pulse train is shown in Figure 4.

The bunch train terminates after 56 pulses, by which time a steady state has almost been achieved. This enables the complete analysis, including transients, to be performed by Laplace transformation. An alternate approach, that would describe only the steady-state response, would be to represent the bunch train by a Fourier series and to use the complex impedance formalism.

As explained in a later figure caption, in order to reduce the computation time (and avoid saturating the figure data sets) the circuit resistance has been artificially increased by a factor of 10, $r_c \to 10r_c$. This only affects the figures. The actual excitation is obtained from the analytic formulas described next.

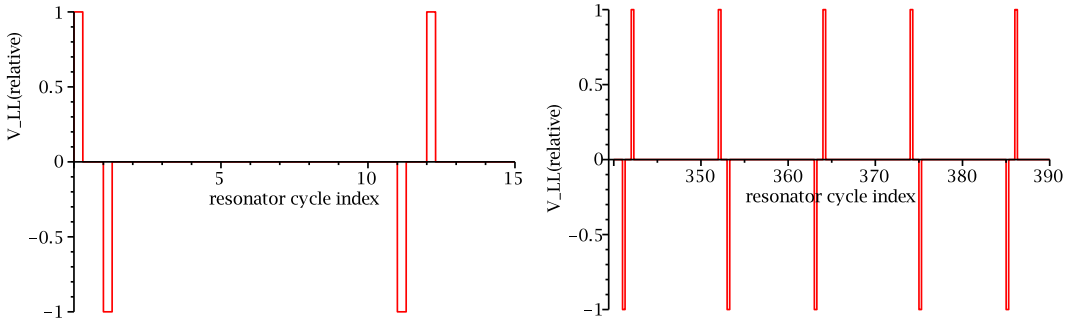

Figure 4: Pulsed excitation voltage pulses caused by successive polarized bunch passages through the resonator. A few initial pulses are shown on the left. The units of the horizontal time scale are such that, during one unit along the horizontal time axis, the natural resonator oscillation phase advances by π. The second pulse starts exactly at 1 in these units, because the resonator length l_c has been arranged so that this time interval is also equal to the bunch transit time through the split-ring. Also, h_c=11 units of horizontal scale advance corresponds to a phase advance of π at the $f_A = f_B = f_0 = 0.2495\,\mathrm{GHz}$ "same-polarization repetition frequency". In other words, 1 unit corresponds almost exactly to 2/11 ns time duration and is a phase advance of π at the $h_c f_0$ polarization repetition frequency and 2π at the $2h_c f_0$ charge repetition frequency. The interval exhibited on the right is a section of the same pulse train plotted with a different horizontal scale, and runs from 340 units to 440 units.

Lumped constant representation of the split-cylinder resonator as a parallel resonant circuit is shown in Figure 5. The resistor symbol is lower case r as mnemonic reminder that we are dealing with a circuit for which inductance L and capacitance C are dominant. The resistor r is taken in series with the inductance under the assumtion that its resistance dominates all other circuit resistances.

The element impedances are given in the figure. The exitation caused by polarized beam passing through the split-cylinder is represented by Lenz law voltage source $\bar{V}_{LL}$, which is the alternating bunch train already described. Voltage division in this series circuit produces capacitor voltage transform $\bar{V}_C(s)$;

$$\bar{V}_C(s) = \frac{1/(Cs)}{1/(Cs) + r + Ls}\,\bar{V}_{LL}(s) = \frac{\bar{V}_{LL}(s)}{1 + rs + CLs^2}. \tag{14}$$

For excitation voltage $V_{LL}(t)$ as shown in Figure 4, MAPLE has been used to determine the Laplace transform $\bar{V}_{LL}(s)$ for substitution into this equation, to obtain $\bar{V}_C(s)$. MAPLE is then used to invert this transform to obtain the capacitor voltage $V_C(t)$, which is plotted in Figures 7 and 8. A short section of the output, superimposed on the input is plotted in Figure 9. Comparing this figure with the early time relation between resonator amplitude and excitation in Figure 6 shows that the response is very nearly in phase with the excitation.

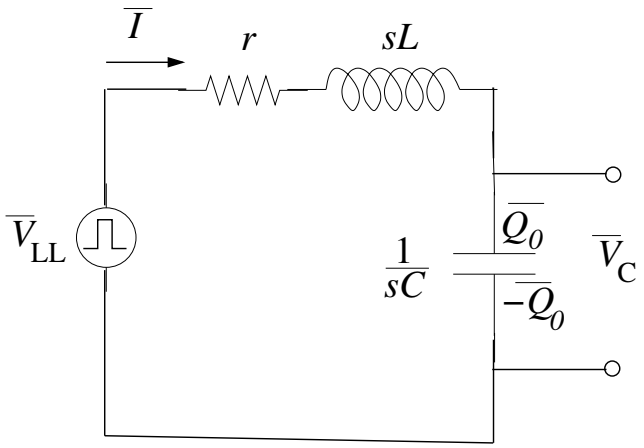

Figure 5: Circuit model for excitation voltage division between capacitance C and inductance L of the resonant LC. The overhead bars on the $\bar{I}$ $\bar{V}$ symbols indicate they represent Laplace-transformed circuit variables.

5 Direct resonator excitation by bunch charge

The alternating polarization of successive bunches moves the resonator response away from the predominant beam charge frequency of $2\omega_c/h_c \approx 0.5\,\mathrm{GHz}$; that is to say, away from even harmonics of the polarization frequency of 0.25 GHz. Nevertheless, each time a single charged bunch passes through the resonator, it produces a small excitation of the oscillator. Even if exactly cancelled by the next bunch passage, this signal exists temporarily. To estimate the importance of this "background" exitation we can assume steady-state resonator response at the level calculated for polarization response and calculate the additionaltransient excitation of the resonator due to the Faraday's law electric field acting on the beam charge. Eq. (11) gives the maximum charge on the capacitor after a single bunch passage to be $Q_1^{\max} = 1.6 \times 10^{-24}\,\mathrm{C}$, which builds up by a factor of $Q_e/h_c = 730$ to a saturation level of $Q_C^{\mathrm{sat.}} = 1.2 \times 10^{-21}\,\mathrm{C}$. From this value, and the "impedance ratio",

$$Z_C = \sqrt{\frac{L_c}{C_c}} = 150\,\mathrm{ohm}, \tag{15}$$

the maximum inductance current can be calculated;

$$I_L^{\mathrm{sat.}} = \frac{V_C^{\mathrm{sat.}}}{Z_C} = 2 \times 10^{-11}\,\mathrm{A}. \tag{16}$$

The corresponding maximum magnetic field is solenoidal, with value

$$B_c^{\mathrm{sat.}} = 5 \times 10^{-16}\,\mathrm{T}. \tag{17}$$

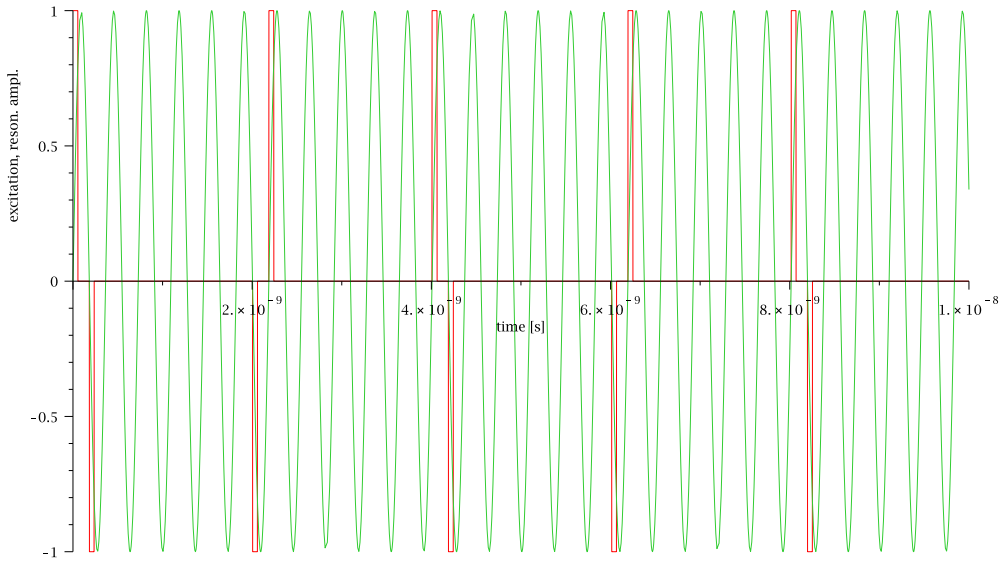

Figure 6: Alternating polarization excitation pulses superimposed on resonator amplitude and plotted against time. Bunch separations are 2 ns, bunch sepraration between same polarization pulses is 4 ns. The vertical scale can represent V_C, E_ϕ, dB_z/dt, or dI_C/dt, all of which are in phase.

At DC there is no work done by the magnetic field on a charged particle. But we are dealing with a time varying magnetic field. In fact the time variation has been intentionally arranged to reverse the magnetic field during the transit time through the split-cylinder. Like the magnetization response, any energy transfers from particle to resonator during entry and exit have the potential for either adding constructively or destructively. Of these we have to identify the excitations that are constructive.

The thin gap in the cylinder is essential for enabling high Q resonance but, otherwise its presence does not significantly influence excitation on a short time scale. This has already been exhibited in the calculation of resonant excitation by beam magnetization, and the same simplification applies for all or most background, direct charge sources.

The current distribution induced by bunch magnetization is purely solenoidal, and the vector potential from a purely solenoidal current distribution is also purely solenoidal. It follows also[3] that, even for a time varying solenoidally field, the electric field is also solenoidal—the only non-vanishing electric field component is E_ϕ.

5.1 On- or off-axis, canted particle incidence

Due to resonator misalignment or beam steering errors the beam centroid may enter the split-cylinder with canted angle, not parallel to the cylinder axis. Without loss of generality we can assume this angle is, say, vertical, $\Delta\theta_y$. For the moment we neglect any impulsive azimuthal velocity occurring in the end field region. If the horizontal entry displacement Δx is zero, there will be no solenoidal component of velocity and no work will be done, by the field on the beam bunch. So we also assume $\Delta x \neq 0$.[1]

[1]Representing the entire bunch as if it is all situated at its centroid is tantamount to neglecting the transverse extent of the bunch and assuming the bunch radius is less than its displacement from the origin. Technically, this

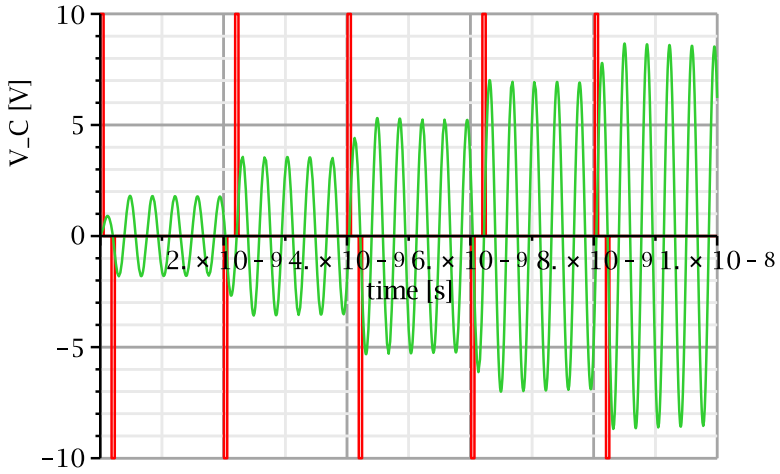

Figure 7: Accumulating capacitor voltage response V_C while the first five linac bunches pass the resonator. The accumulation factor relative to a single passage, is plotted.

For symplicity we also suppose the orbit is aimed vertically to cross the horizontal design plane $y = 0$ at the longitudinal $z = 0$ center of the resonator. The equation of the orbit path through the resonator is then

$$\begin{aligned} x &= \Delta x, \\ y &= -\Delta\theta_y z = -\Delta\theta_y v_e t, \end{aligned} \tag{18}$$

where v_e is the particle (almost exactly longitudinal) velocity. Meanwhile, using Faraday's law, the solenoidal magnetic field, magnetic flux φ through a centered circle of radius Δx and the corresponding e.m.f. are given by

$$\begin{aligned} B_z &= B_c^{\text{sat.}} \sin(\omega_c t + \psi), \\ \varphi &= \pi \Delta x^2 B_c^{\text{sat.}} \sin(\omega_c t + \psi), \\ \text{e.m.f.} &= -\frac{d\varphi}{dt} = -\pi \Delta x^2 B_c^{\text{sat.}} \omega_c \cos(\omega_c t + \psi) \end{aligned} \tag{19}$$

where ω_c corresponds to the $h_c f_0 = 2.7\,\text{GHz}$ frequency with which the resonator is oscillating and ψ is a possible phase shift of the particle bunch arrival time relative to the resonator phase. (The time dependence of B_z has been expressed as $\sin(\omega_c t + \psi)$ (rather than cosine) because B_z is "in quadrature" with, for example, V_c, which can be seen in Figure 6 to be sine-like at the time origin. More on the phase issue later.) The beam bunch is subject to a Faraday's law electric force given by

$$F_y = N_e e\, E_\phi = N_e e\, \frac{\text{e.m.f.}}{2\pi\Delta x} = -\frac{1}{2}\, N_e e \Delta x B_c^{\text{sat.}} \omega_c \cos(\omega_c t + \psi). \tag{20}$$

assumption becomes invalid once the bunch displacement is less than the bunch radius, which will always be the case once the line is properly tuned. But the approximation actually remains good even in this limit, especially with the beer-can bunch shape. The displaced bunch can be replaced by a perfectly centered circular distribution (which does no work) plus two "lunes" (i.e. new-moon-shaped crescents) one with positive charge density, one negative. The fraction of total charge in each lune is approximately $\Delta x/r_c$. Representing each lune by a point at $x = r_c$ magnifies the work by a factor of roughly $0.5 r_c/\Delta x$, compared to its being located at $x = \Delta x$. The work done on the two lunes is twice the work on the positive density one. All of this is equivalent to pretending $r_c << \Delta x$, in spite of the fact that r_c is actually greater than Δx.

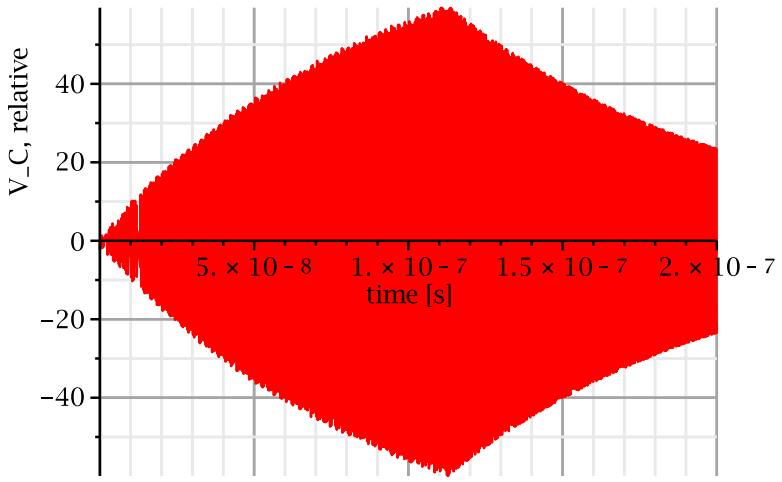

Figure 8: Relative resonator response to a train of beam pulse that terminates after about 110 ns. (The Laplace transform formalism requires the time duration of the excitation to be finite.) After this time the resonator rings down at roughly the same rate as the build-up. With just one exceptions the circuit parameters are those given in Table 1. The exception is that the resistance for the plot is $r = 10r_c$. The true response build up would be greater by a factor of 10, over a factor of 10 greater build-up time.

(With the vertical motion being non-relativistic) the work done on the bunch during vertical displacement $v_e\Delta\theta_y dt$ is $dW^{\rm m.a.} = F_y v_e \Delta\theta_y dt$ and the total work done during a single bunch passage is given by

$$W_1^{\rm m.a.} = -\frac{1}{2}\,\frac{N_e e\omega_c}{\omega_c}\,v_e\Delta\theta_y\Delta x B_c^{\rm sat.}\int_{-\pi/2}^{\pi/2}\Big(\cos\omega_c t\cos\psi - \sin\omega_c t\sin\psi\Big)d(\omega_c t). \tag{21}$$

The integral evaluates to $2\cos\psi$, and the ratio ω_c/ω_c can be replaced by $2f_0/2f_0$ to permitt the factor $N_e e 2f_0$ to be replaced by the proposed average injection line beam current $I_{\rm ave} = 160\,\mu$A.

$$\boxed{W_1^{\rm m.a.} = -\left(\frac{I_{\rm ave}}{2f_0}\,v_e B_c^{\rm sat.}\,\frac{1}{r_c}\right)\Delta\theta_y\Delta x\cos\psi = -\Big(4.5\times10^{-20}\,{\rm J/m}\Big)\,\Delta\theta_y\Delta x\cos\psi.} \tag{22}$$

Like Eq. (12, this equation is boxed to emphasize the importance of comparing "background" $W_1^{\rm m.a.}$ with "foreground" $U_1^{\rm pol.}$. The superscript on $W_1^{\rm m.a.}$ is an abbreviation for "misalignment". With perfect, time-independent positioning of the resonator $W_1^{\rm m.a.}$ would vanish, which would clearly be unrealistic.

The arbitrary phase angle ψ was introduced earlier, in connection with Eq. (12). The dependence on phase factor $\cos\psi$ makes is strongly advisable to include phase sensitive detection as and aid in distinguishing foreground from background. This is the significance of the $\cos\psi$ factors in the boxed equations. It will be important to confirm that these factors are, in fact, the same, rather than being out of phase, for example, by π, which would be the case if one of these factors were replaced by $\sin\psi$.

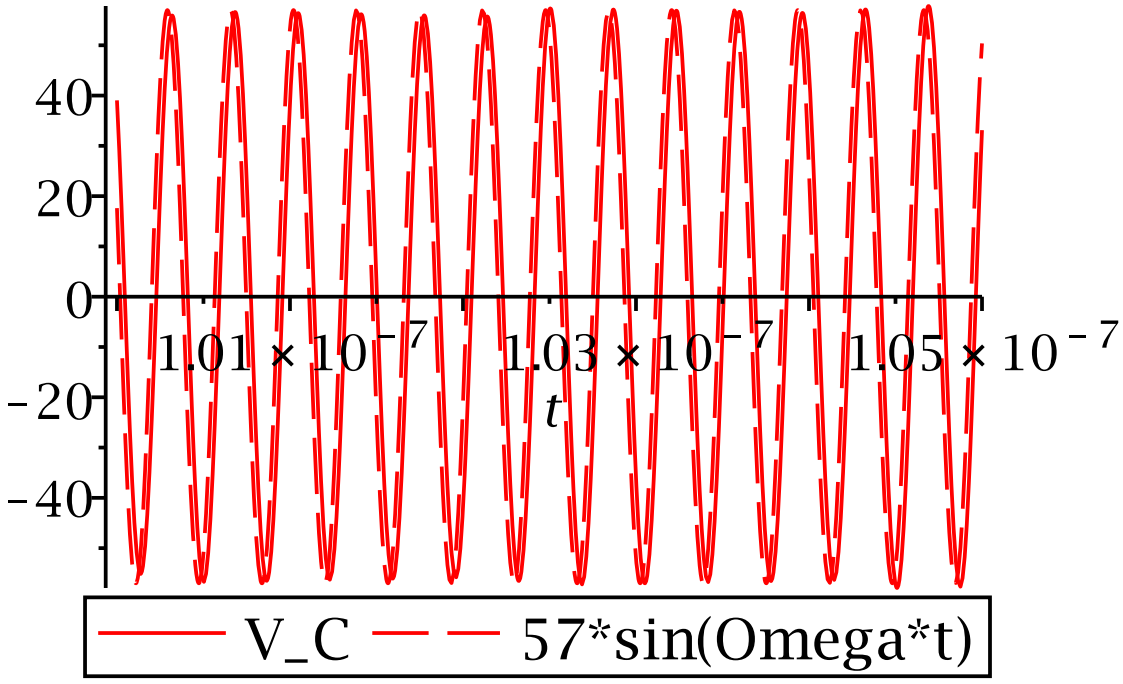

Figure 9: Phases of drive and response (in the form of capacitor voltage V_c) after 100 ns. Surprisingly, the response is almost in phase with the excitation. This is presumeably because the entrance and exit excitations are separated in phase by π.

5.2 Off-axis, parallel particle incidence

Consider, next, a beam bunch approaching the solenoid parallel to the cylinder axis. The longitudinal magnetic field can be expressed as $B(z)\hat{\mathbf{z}}$ where $B(z)$ varies from $B(z-) = 0$ outside to $B(z+) = B_0$ inside. The full magnetic field can be approximated as

$$\mathbf{B} = \frac{-dB(z)/dz}{2}\, x\hat{\mathbf{x}} - \frac{dB(z)/dz}{2}\, y\hat{\mathbf{y}} + B(z)\hat{\mathbf{z}}, \tag{23}$$

where $B(z)$ is a function varying over a short z-interval, from a constant value of 0 outside to a value of B_0 inside. The $\nabla \cdot \mathbf{B} = 0$ vanishing divergence condition can be seen to be satisfied. The function dB_z/dz is strongly peaked at the solenoid entrance and exit, and can be approximated by the sum of two δ-functions. As a result

$$B_x(z) = B_y(z) = -\frac{1}{2}\frac{dB_z}{dz} \approx \frac{-B_0}{2}\Big(\delta(z + l_c/2) - \delta(z - l_c/2)\Big), \tag{24}$$

where B_0 is the constant, longitudinal, internal magnetic field. An electron initially traveling in the horizontal $y = 0$ design plane, along a line at constant $x = \Delta x$, impulsively acquires an azimuthal (vertical) velocity Δv_y at the entrance satisfying

$$m_e\gamma_e\Delta v_y = \int_{-l_{c-}/2}^{-l_{c+}/2} ev_e\hat{\mathbf{z}} \times B_x(z)\hat{\mathbf{x}}\Big|_y\, dt = \int_{-l_{c-}/2}^{-l_{c+}/2} \frac{B_0}{2}\delta(z + l_c/2)\, d(v_e t) = \frac{eB_0}{2}. \tag{25}$$

This agrees with Kumar's Eq. (5)[4]. Solving this equation for Δv_y with resonant split-ring resonator parameters, the vertical angle $\Delta\theta_y$ is given by

$$\begin{aligned}\Delta\theta_y = \frac{\Delta v_y}{v_e} &= \frac{cB_c^{\text{sat.}}}{2\beta_e\gamma_e m_e c^2/e}\,\Delta x \\ &= \frac{(3\times10^8)(5\times10^{-16})}{(2)(0.866)(2)(0.511\times10^6)}\,\Delta x \\ &= 0.85\times10^{-13}\,\Delta x. \end{aligned} \tag{26}$$

This radial deflection initiates a helical motion, but the particle stays in the cylinder only for a time of duration l_c/v_e, which is not long enough for any motion other than in the y-direction to develop.

The value of $\Delta\theta_y$ given by Eq. (26) can be compared with the same angle $\Delta\theta_y$, taken in the previous section as an input parameter representing the vertical cant angle of the incident beam. (As in that equation, except for the small cant angle under discussion, because of azimuthal symmetry, the orbital azimuth was taken to be approximately horizontal without essential loss of generality.)

The extreme smallness of the coeficient in Eq. (26) is due to the extremely weak magnetic field factor. One sees that the work on any particle entering the solenoid parallel to the cylinder axis, can be neglected, irrespective of its transverse position. For subsequent discussion it is only the work $W_1^{\text{m.a.}}$ given by Eq. (22) that needs to be taken into account.

5.3 Why random phase? Why helicity? Why quantum mechanics?

The results from the previous two sections have validated ignoring the effect of the resonator magnetic field on the particle orbit. Each particle, and therefore also the bunch centroid, can be treated as following a straight line through the split-cylinder. The sign of the instantaneous work being done on a particle by the resonator boils down to the question of whether the dot product of the Faraday's law electric field vector with the particle's velocity vector is positive or negative. (Because the Faraday's law electric field vector is exactly azimuthal) this boils down to whether the "effective helicity" of the particle (or bunch centroid) is positive or negative. Here "effective helicity" is an ad hoc (temporary) property describing whether the paricle trajectory is related to the resonator axis as a left-hand or a right-hand screw. (If, viewed with particle approaching, the particle line is sloping up as it misses the resonator axis on the right, then the particle advance is like that of a right-hand screw, etc.)

A possible background suppression mechanism relates to the $\cos\psi$ factors appearing in boxed Eqs. (12) and (22). The $\cos\psi$ factor has been referred to as a "random phase factor". (Especially at GHz frequencies) it is difficult to define, much less measure, the phase angle ψ. It is only rarely possible to measure it in practice. As a practical matter, it is possible only to measure the difference $\Delta\psi$ between two sinusoidally-varying amplitudes being measured at the same point.

As it happens, our apparatus, which responds synchronously to foreground (magnetization-excitation) and background (charge-excitation) is one such instance. This would *not* be the case with perfect beam set-up in which the charge excitation is limited to even harmonics of f_0 and the resonator is tuned to an odd harmonic of f_0. Rather, we are concerned with improperly balanced A and B bunches which lead to charge excitation at odd harmonics of f_0—in particular the $h_c = 11$ odd harmonic to which the resonator is tuned.

To understand this distinction one can consider the most extreme possible example of sub-harmonic beam current frequency leakage from $2f_0$ to f_0. Let us suppose one or the other of the A and B beams is turned completely off, without affecting the other. On paper, this can be done exactly. We idealize by assuming it can be done to very high precision in the real world. Then the

beam current frequency spectrum is purely sub-harmonic, at f_0 and all of its harmonics—including, in particular, $h_c = 11$. In this configuration the background charge excitation caused by, say the A beam, closely mimics the excitation of perfectly balanced, interleaved, opposite-polarization, A and B beams. (We return later to analyse this configuration for operational alignment of the resonator and beam steering by nulling the responses of A and B beams separately.)

Consider the passage through the resonator of just one of the beam bunches, assumed to be short compared to the transit time. For maximum net work to be done during transit, say on a right-handed particle trajectory, the Faraday electric field E_ϕ polarity should not change sign during the transit. The sign of the work will be the same as the Faraday polarity. On the other hand, for the beam magnetization excitation to be maximal, the capacitor voltage V_C must not change sign during transit. (See Figure 6.) As indicated in the caption to Figure 2, E_ϕ and V_C are synchronous or, at least, *not in quadrature*. (Depending on sign convention, they may be out of phase by π, but not by $\pi/2$.) This means that it has been self-consistent for the $\cos\psi$ factors to be the same in both of the boxed equations.

By causing the beam centroid to pass exactly along the axis of the resonator, or with all orbits exactly parallel to the resonator axis we would exactly eliminate the charge-excitation. Of course we cannot achieve either of these things exactly, but that is what has to be attempted.

Our efforts to measure the magnetization of a bunch of particles is greatly simplified by the fact that the bunch contains 2×10^6 particles. Even with such large charge, it is difficult for the resonator excitation to be visible above the thermal noise floor. From our theoretical estimates so far, it is clear that it would be impossible to detect the excitation of any macroscopic resonator by the passage of a single electron. But, if the resonator were a single atom or molecule, with long-lived excited state, it is presumeably possible to detect transition from ground state to excited state. Of course this can only be analysed quantum mechanically. But it should not be surprising that the excitation depends on the electron helicity.

As already mentioned, most accelerator beam position or beam current monitors are not capable of resolving quadrature components separately (for example because no absolute phase reference signal is available). But within the telecommunications field it is standard practice to resolve these components. This does, however, require phase sensitive detection, which requires, in turn, a very stable trigger pulse train synchronized with the beam pulse arrival times. This should be available for the CEBAC injection line. It seems that such detection is likely to be possible. Regrettably, as we have seen, our background and foreground signals are *not in quadrature,* so synchronous detection will not automatically enable us to separate background from foreground. Nevertheless, we continue to investigate ways in which synchronous detection can be useful.

Based on our new emphasis of "effective helicity", in order to better analyse background rejection, we copy, and modify slightly, misalignment-excitation formula (22),

$$\boxed{W_1^{\text{m.a.}} = -\left(\frac{I_{\text{ave}}}{2f_0}\, v_e B_c^{\text{sat.}} \frac{1}{r_c}\right) \Delta\theta_\perp |\Delta\rho|.} \tag{27}$$

All that has been done has been to switch from transverse Cartesian (x, y) coordinates to transverse cylindrical $\big(\Delta\rho, \varphi\big)$ coordinates. The radial coordinate has been expressed as $\Delta\rho$ to emphasize its smallness and (redundantly) been expressed as absolute value, to emphasize that radii are always positive. By symmetry, the aximuthal angle φ does not actually appear in Eq. (27). Also the subscript on cant angle $\Delta\theta_\perp$ indicates that this angle is *perpendicular to* the plane containing the cylinder axis and the point of nearest approach. Though exactly equivalent to Eq. (22), Eq. (27), is intended to make it clear that only one of the differentially-small quantities can change sign. This is related to the fact that a cant angle $\Delta\theta_\parallel$ (parallel to the same plane) causes no resonator excitation. Though it is not conventional terminology, for mnemonic purposes, the quantity $\Delta\theta_\perp|\Delta\rho|$ can be referred to as a"effective helicity".

Our problem in tuning away the background charge excitation is not unlike the quantum mechanical problem. When the centroid is very nearly aligned, the effective helicity has been nulled very nearly to zero, but of one sign or the other. The tiniest of steering changes cause the effective helicity to reverse, which causes the sign of the excitation to reverse. One hopes to exploit this feature for tuning purposes.

6 Coaxial signal combination with quadrature cancellation

Because the magnetization-induced resonator excitation is so weak it will be highly advantageous to be able to coherently add the excitation amplitudes from more that one, for example, let us say, $N_d = 8$ separate transducers. (Some ways of combining signals are mentioned in an appendix.) For the same reason, because the direct beam charge-induced resonator excitation is potentially much greater than the magnetization-induced excitation, it is important for the transducer to be as insensitive as possible to the passage beam charge.

The alternating polarization of successive bunches has already provided one stage of background rejection by "eliminating" the beam current frequency content at all odd harmonics of f_0, while assuring that the magnetization spectrum consists of all harmonics of f_0—including, in particular, the 11'th harmonic at frequency $f_c = h_c f_0 = 11 f_0$.

The circuit shown schematically in Figure 10 has been designed both for signal magnification and to help in foreground/background separation. More physical representations of the same apparatus are shown in Figure 11. Because lumped-constant (crude approximations) are being combined with distributed-constant (more reliable approximations) the following discussion has to be qualified as only being semi-quantitative.

As explained already, a longitudinally-polarized beam bunch passing through the split-cylinder causes a small charge $Q_1^{\max}$ given by Eq. (11) to be deposited suddenly on the capacitor C_c. As can be seen in Figure 10, the sudden appearance of this charge, applies a voltage impulse δV to the transmission line at the capacitor location. Traveling waves of amplitude $\delta V_+ = \delta V_- = (1/2)Q_1^{\max}/C_c$ are launched in the positive and negative directions along the transmission line.

The phase velocity of the coaxial transmission line has been arranged to be exactly equal to the velocity of the electron beam. As a result, the beam bunch under discussion arrives at the next capacitor along the beam line at exactly the same time as the amplitude maximum of the wave corresponding to the previously-introduced δV_+ pulse. This bunch passage produces another forward-going and another backward-going voltage pulse on the line. Temporarily ignoring the backward-going pulses that are being produced, and assuming perfect coherence, after passing N_d successive resonators, a forward going wave of amplitude corresponding to charge $N_d Q_1^{\max}/2$ will have been produced. This forward-going wave proceeds towards the receiver, where it is absorbed without reflection in the pure resistor R_0, whose value is equal to the characteristic impedance Z_0 of the line.

We are neglecting the small impedance mismatch occurring at the location along the line where the periodic loading stops and unperturbed coax begins. The validity of this assumption is investigated in Appendix A. This defect could, if necessary, be avoided by appropriate impedance matching.

The backward-traveling pulses do not have very far to go before they come to the upstream end of the transmission line. The waves are reflected with the same amplitude, but with sign depending on the setting of the switch at this location. Treated as waves, the wave phase is unshifted with the line open at the end, but shifted by π with the line short-circuited.

In either case, because the length of the cable extension beyond the upstream end of the first split-cylinder is equal to $\lambda/4$ (or half the free length between split-cylinders) each previously-upstream-traveling, now downstream-traveling bunch will interfere coherently (constructively or

destructively or, possibly, something in between) with pulses being produced by the beam bunch number $N_d + 1$ (where the previously-analysed bunch is number 1).

One sees, therefore, that the multi-element array can act as a kind of "phase-sensitive transducer" (for waves whose origins are spatially-synchronized with the signal transducers). Consider a backward wave initiated at the A/B site. (The points A and B are located just before and just after the resonator connection. This distinction is important in Appendix A, but unimportant for the present discussion.) If the coax is open at its upstream end, there is no phase shift of the backward-traveling wave initiated at A/B as the wave is reflected and becomes forward-traveling. On its return to the A/B point, after traveling an integral number of λ lengths, this wave will interfere constructively with the already forward-traveling waves on the line. On the other hand, if the upstream end of the coax is short-circuited, the interference will be destructive. In this latter, shorted-end, case, the overall destructive interference will cause no net polarization-induced signal to appear at the receiver.

Let us suppose, therefore, that the upstream end of the coax is open-circuited, and consider a wave emanating from location C, which is displaced by $\lambda/4$ from A/B. With the coax open-circuited, on its return to location C, this wave, after reflection, will have traveled an odd number of half-wavelengths, and suffered no phase shift. The net result, in this case, will be zero net receiver signal.

The previous few paragraphs have justified our use ot the term "phase-sensitive transducer" to describe the proposed apparatus. As already acknowledged, since circuit and wave concepts have been mixed, these, and (especially) subsequent conclusions based on this concept, will have to be confirmed using more self-consistent analysis and, especially, by experimental confirmation. But, we will proceed as if this confirmation has already been successfully accomplished.

It is disappointing that the foreground and background signals are not in phase quadrature. If they were, their separation would be clean. Instead we have to figure out ways to use this tail for further background reduction.

7 Operational beamline tuning for background suppression

Other than depending on energy, and being proportional to both beam polarization and beam current, "foreground" resonant excitation induced by the beam polarization is quite insensitive to beamline design. However, the successful detection of beam polarization will rely on the extreme selectivity required to adequately suppress the "background" due to direct excitation by the beam charge.

It is not at all realistic to assume perfect cancellation of the f_0 frequency component of beam current by the careful interleaving of A and B beams. Without care the currents of the CEBAF A and B bunches, which arrive alternately at the resonator, may be different, by one percent, for example, which would cause the the overall beam current to have an approximately half percent frequency component at the f_0 frequency of the individual A and B beams.

To represent the degree of leakage of beam current from the design $2f_0$ beam charge frequency to the f_0, sub-harmonic frequency, one can define a ratio

$$\eta^{\mathrm{sub-harm.}} = \frac{I_{f0}}{I_{2f0}}. \tag{28}$$

Ideally the value of this ratio would be zero. The unintended I_{f0}-induced resonator excitation will be subject to the same resonant magnification as the polarization component. This will be the significant source of spurious, polarization-mimicking background. For conservative planning, operational procedures to reduce the $\eta^{\mathrm{sub-harm.}}$ factor to a confirmably small value need to be identified.

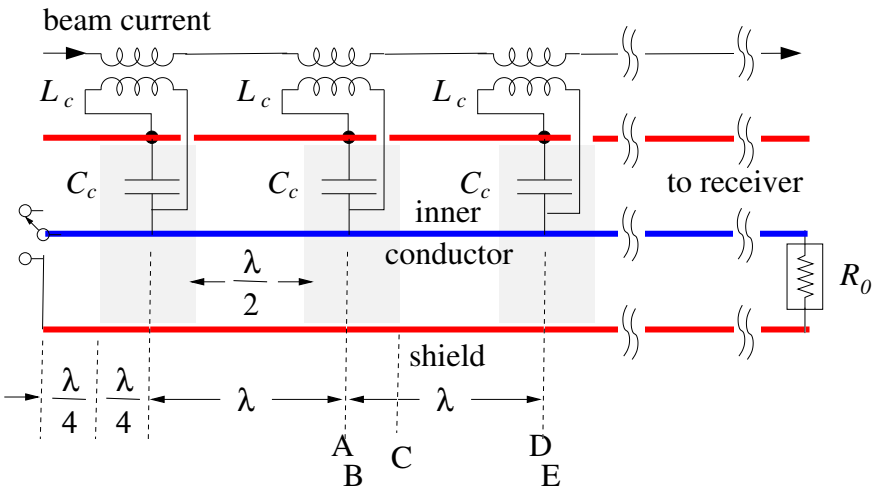

Figure 10: Circuit diagram for a circuit that sums the signal amplitudes from sequential polarimeter resonators on a transmission line leading from polarimeter to receiver. Just three pick-up locations are shown, but four or eight (as assumed in the text), or other numbers of cells would be practical. The beam tube itself is not shown, but the longitudinal extent of the split cylinders are indicated by shading. The capacitors are not actually inside the coax—they are drawn there only to help make it clear pictorially that the capacitor C_c and inductor L_c "look" to the transmission line like "loading" by a parallel resonant circuit. Excitation by passing beam bunches is represented by inductive coupling. The polarization wave moves from left to right in the coax at the same speed as the beam in the beam tube. The receiver end is terminated in the characteristic resistance R_0 of the coaxial line. Depending on the upstream switch position, to open or short circuit, one or the other quadrature amplitude component is added constructively or destructively. The label pairs A,B and D,E represent points electrically just before and just after the resonator connection.

7.1 Simplifying features and assumptions

Discussion of background suppression can be simplified by taking advantage of reasonable simplifying assumtions:

1. As just mentioned, though foreground resonant excitation depends critically on the resonator design, the foreground response is largely independent of beamline imperfections. This includes independence from resonator positioning imperfection and independence from (even time dependent) errors in transverse beam position and beam angle, both horizontally and vertically. It is only for background suppression that the beam and cavity positioning and alignment is critical. Nulling of the sub-harmonic charge excitation can proceed without worry about the influence on the magnetization excitation.

2. Though highly sensitive to beam and cavity positioning, the main background signal (i.e. the sub-harmonic frequency leakage from $2f_0$ to f_0 is constrained by the $\Delta\theta_\perp|\Delta\rho|$ factor in Eq. (27).

3. By design, the beam current (irrespective of polarization) is perfectly periodic, with period $T_{A+B} = 1/(2f_o)$—it is the exact identity, in all respects (except for half-period delay) of A and B bunches that provides this perfect periodicity. The ideal frequency beam current spectrum then contains only even harmonics of f_0. The entire success of resonant polarimetry depends on the degree to which this beam idealization is met.

4. Of course the A and B bunch charges will not, in fact, be exactly equal. This is the simplest imperfection to describe, and the most important operational background suppression will probably come from minimizing this beam current imbalance at the source.

5. The transverse A and B betatron orbits will also not be identical. But, from what has been assumed already, it is only the effective helicity of their sub-harmonic frequency leakage that needs to be canceled.

6. Cancelling the sub-harmonic f_0 spectral component of beam current is being emphasized in this section above all other background suppression issues for only one reason. Beam current excitation at this frequency will be subject to the same resonant amplification, by as much as four orders of magnitude in amplitude, as is the magnetization excitation. Other background error sources will not be magnified in this way. One must strive therefore, to suppress the sub-harmonic beam current leakage from $2f_0$ frequency to f_0 by a factor of about 10^4 in amplitude. Discussion of this point in more detail is continued in following sections where operational suppression measures are described.

7.2 Cancellation of beam charge frequency leakage $2f_0 \rightarrow f_0$

The basic balancing meachanism of A and B beam currents will probably be done by stabilizing the two separate laser source intensities. Stabilization mechanism to do this are assumed to exist already. Tuning steps specific to resonant polarimetry follow:

1. Using a beam current monitor (BCM) located downstream near the resonant polarimeter, the f_0 half-frequency response can be fed-back as laser intensity control inputs to refine the $2f_0 \rightarrow f_0$ beam current cancellation.

2. Two pairs of very weak and appopriately spaced transverse beam shakers, one horizontal, one vertical, can be located (appopriately spaced) at the same location, just far enough upstream from the polarimeter (say 1 m to 2 m upstream) to produce transverse position and slope modulations of the beam, both horizontal and vertical.

3. Each of these four shakers has to have both accurately controllable DC adjustment (for steering) and (not particularly precise) RF amplitude adjustment (for shaking).

4. Since diagnostic information using this beam shaking will come from sidebands of f_0, the shaking frequency has to be at a frequency large enough (say $f_{\rm mod}$=several MHz) to be substantially larger than the value shown in Table 2 in the row labelled "min. modulation freq.". Let us consider just the horizontal beam shaking—everything can be simply repeated for the vertical shaking.

5. To the extent the configuration is misaligned the sub-harmonic f_0 beam current background component (presumeably much reduced already, compared to the $2f_0$ dominant beam current component) will acquire side-bands at frequencies $f_0 \pm f_{\rm mod}$. These have to be resolveable from the "carrier signal" at f_0.

6. Because of the $\Delta\theta_\perp|\Delta\rho|$ constraint, the horizontal position and vertical slope should be nulled together. And, after that, the vertical position and horizontal slope. This can be done first with unpolarized A and B beams individually (with huge side-band signals expected). Then, later, with unpolarized, but optimally-superimposed A and B beams (with weak side-band signals expected).

7. The nulling so far has use only unpolarized beams. But the side-band response can also be nulled even with polarized beam, without nulling the polarization signal. As explained

earlier, the polarization response is independent of both polarimeter position and angular dispacement. Of course, with polarized beam, it is only the side-bands that are to be nulled, whatever signal remains at the central $2f_0$ is to be interpreted as being induced by the beam magnetization.

8. As mentioned already, the same operational procedures have to be performed iteratively between horizontal and vertical.

9. Conventional $BPMs$ downstream of the transverse shakers just introduced, and tuned to either the unintentional $2f_0$ current component or to the intentional $2f_0$ beam frequency, will also exhibit modulation sidebands. But these side-band responses will be due to the betatron positional displacements at their positions rather than to betatron angles. Nevertheless any sideband responses at $2f_0$ would indicate the presence of beam imperfection that is potentially capable of producting background resonator excitation that would be erroneously attributed to beam polarization.

7.3 Foreground/background frequency separation by parameter modulation

Another possible way of improving the rejection of direct charge excitation has been much discussed in the past, though not yet in this paper. Instead of the beam polarization being steady, it can be modulated at a low frequency in the KHz range. Before discussing this topic a more straignt forward exploitation of the quadrature relationship between foreground and background will be considered.

7.3.1 Source polarization modulation

7.3.2 Beam deflection

Not yet written.

8 Recapitulation and conclusions

For resonator parameters shown in Table 1, the maximum charge $Q_1^{\text{sat.}\cdot}$ residing on the resonator capacitor when the first bunch has just entered the resonator was determined in Eq. (11). Figure 7 shows the capacitor charge building up constructively over the next several excitation pulses. The synchronism has been arranged so that every entrance and exit Lenz law excitation is constructive. Multiplying V_C by 10 in Figure 8 (to correct for the actual circuit resistance r_c having been artificially increased by a factor of 10 to reduce the computation time) the capacitor build-up factor when steady state has been reached is approximately 700. This is less than the resonator Q value of 8031 by a factor more or less equal to the $h_c = 11$ resonator harmonic number. Accepting this ratio, at that time the capacitor charge is $700\, Q_1^{\text{sat.}\cdot} = 1.6156 \times 10^{-24} = 1.1309 \times 10^{-21}$ C, and the saturation capacitor voltage is

$$V_C^{\text{sat.}\cdot} = \frac{(Q_c/h_c)\, Q_1^{\text{sat.}\cdot}}{C_c} = \frac{(8031/11)\cdot(1.1309\times 10^{-21})}{0.4032\times 10^{-12}} = 2.926\times 10^{-9}\,\text{V}. \tag{29}$$

Accepting the multi-element polarimeter circuitry described in Section 6 as feasible in every respect, the voltage at the receiver will be increased by a factor equal to the number of pick-ups, which we have tentatively taken to be $N_d = 8$. The receiver voltage will then be

$$V_C^{\text{rcvr.}\cdot} = \frac{N_d(Q_c/h_c)\, Q_1^{\text{sat.}\cdot}}{C_c} = 6.637\times 10^{-8}\,\text{V}. \tag{30}$$

For data collection intervals of order one second, this signal can be expected to be well above the thermal noise floor and other environmental noise sources. Even if background and foreground signals are comparable in magnitude, numerous operational tuning mechanisms have been described for the further isolation of the foreground magnetization signal, which yields the beam polarization, from the background signal.

As an aside, one can comment that, since the electron velocity of $0.866\,c$ is almost fully relativistic, this voltage is very nearly independent of γ. As far as I am concerned this lays to rest a decade old controversy concerning the γ-dependence of cavity excitation by a passing bunch of polarized particles. This paper has shown that, once the particles have become fully relativistic there is no further dependence on γ of the resonator excitation.

9 Appendices

A Wave propagation on a periodically-loaded coaxial line

Not yet written.

B Frequency choice considerations

My recommended multi-element design has already been described in Section 6. It may be worth considering other frequency choices. This section considers other (less-esoteric) ways of increasing the signal strength by combining the signals from multiple resonators. The feasibility of doing this very much depends on the choice of resonator frequency. (Especially at very low electron energies) the overall length of beamline available restricts the number of elements that can be inserted in the beam line. This consideration greatly favors high frequencies, such as the $f_c = 2.7445\,\mathrm{GHz}$ resonator frequency emphasized in this paper. Figures 11, 13, and 12 illustrate the following discussion.

Because the individual resonators are so short, especially at the highest frequency, it will be practical to line up several identical resonators, for example $n_{\mathrm{cells}} = 8$, appropriately spaced, and let the beam pass through them in sequence. Assuming the resonators are physically identical, and they are identically aligned, their RF exitations will be identical. Added with perfectly constructive interference, the signal power would be increased by a factor $n_{\mathrm{cells}}^2 = 64$. As well as improving the signal relative to thermal noise ratio, a big signal amplitude increase like this would greatly reduce the importance of extraneous noise sources.

The circuitry for combining the multiple resonator outputs seems to be straight forward. Some circuit possibilities are shown in Figure 12.

The paper so far has analysed only $h_c = 11$ as the choice of harmonic number. To diccuss the choice of frequency, parameters for other harmonic number choices, $h_c = 9.7, 5, 3, 1$ are given in Table 2. This provides resonator frequency choices from $f_c = 0.2495\,\mathrm{MHz}$, to $2.7445\,\mathrm{MHz}$. For any particular choice of frequency, the first parameter to be fixed is l_c, to match the transit time to the appropriate π phase advance. With cylinder radius r_c held constant, the inductance L_c is fixed, leaving the capacitance-sensitive parameters w_c and g_c as the only remaining free variables. (In fact even the presence of ring wall thicknes w_c is artificial in that using the parallel-plate capacitance formula is far from being valid.) Except for this capacitance choice, fixing h_c essentially fixes all resonator parameters. With multiple resonators the drifts lengths scale scale proportionally.

The highest frequency case, $h_c = 11$, is optimaal from some points of view, and especially for multiple resonator signal amplification. With $n_{\mathrm{cells}} = 8$ overall length would be $L_{\mathrm{tot.}} = 2n_{\mathrm{cells}}l_c = 16 \times 0.04733 = 0.76\,\mathrm{m}$.

Highest frequency can also be seen to be best for maximum resonator quality factor Q_c. However the "effective Q" res. fac. $= Q_c/h_c$ favors low frequency. What makes this dependence important is that the foreground energy signal is proportional to $(Q_c/h_c)^2$,

A parameter that will be important is the modulation range, f_c/Q_c. In order for modulation to comfortably support frequency domain separation of foreground and background excitations, the modulation has to exceed this modulation range parameter. This parameter also favors low frequency.

These considerations may eventually change the choice of resonant frequency. But the favored design described in Section 6 strongly supports Brock Roberts's choice of harmonic number $h_c = 11$ for sdetermining the resonator frequency.

These considerations would be different for polarized proton polarimetry, because of the much longer bunch lengths, and therefore much longer resonator, and lower frequencies. Because of frozen spin protons would be much stiffer than the $\gamma = 2$ electrons considered in this paper, the resonators could be much longer and the beams more intense. Achieving satisfactorily high resonator Q-values might, then, require cryogenic resonators.

parameter	unit	value						
cav. harm. num.	h_c		1	3	5	7	9	11
resonant freq.	f_c	GHz	0.2495	0.7485	1.2475	1.7465	2.2455	2.7445
min. modulation freq.	f_c/Q_c	KHz	103	178	230	273	309	342
quality factor	Q_c		2421.3	4193.9	5414.3	6406.3	7264.1	8030.7
reson. ampl. fact.	M_r=Q_c/h_c		2421.3	1398.0	1082.9	915.2	807.12	730.07
detune per deg C	$T_{\text{coeff.}}Q_c$	1/degC	0.0410	0.0712	0.0920	0.1090	0.1234	0.136
cylinder length	l_c	m	0.5206	0.17354	0.10412	0.07437	0.05785	0.04733
cylinder radius	r_c	m	0.01	0.01	0.01	0.01	0.01	0.01
gap height	g_c	mm	0.02849	0.1480	0.31853	0.5277	0.7693	1.0394
wall thickness	w_c	mm	3.3166	1.9149	1.4832	1.2536	1.1055	1.0
capacity*	C_c	pF	536.62	19.875	4.2930	1.5644	0.73611	0.40317
inductance	L_c	nH	0.7583	2.2748	3.7914	5.3080	6.8245	8.3411
res. imp. fac.	$\sqrt{L_c/C_c}$	ohm	1.189	10.70	29.72	58.25	96.28	143.83
skin depth	δ_s	μm	4.130	2.3844	1.8469	1.5610	1.3766	1.2452
eff. resist.	R_c	ohm	0.00491	0.002551	0.005488	0.009092	0.01326	0.017911
bunch freq,	f_0	GHz	0.2495	0.2495	0.2495	0.2495	0.2495	0.2495
cav. trans. time	Δt	ns	2.005	0.66843	0.40106	0.28647	0.22281	0.18230
trans. cycle adv.	$\Delta\phi_c$		0.5003	0.5003	0.5003	0.5003	0.5003	0.50032

Table 2: Parameters for all electron EDM sensitive split-cylinder resonances with frequency less than 3 GHz (i.e. odd harmonic numbers $h_c \leq 11$). Highest frequency is most favorable for foreground/background response. The cylinder length l_c is fixed by the cavity transit time condition, and the cylinder radius $r_c = 1\,\text{cm}$ is arbitrarily held constant. But the capacity-determining parameters g_c and w_c have been scaled from the $h_c = 11$ case analysed so far, and are not necessarily physically sensible, especially at the low frequency $h_c = 1$ extreme. *Other compromises between g_c and w_c may be preferable, including the possibility of increasing the capacity by high permittivity spacer such as sapphire in the gap or external capacitor.

C Frequency tuning and temperature compensation

Possible mechanical design features for combining signals with the $h_c = 11$ frequency option are shown in Figures 11, 13, 12. The need for temperature compensation can be inferred from the "detune per deg" column of Table 1. The dependence of resonance frequency on temperature is most severe at highest frequency. For these entries the resonator is assumed to be free and unconstrained. The entry 0.136 indicates that a one degree change in Celsius temperature (assuming

copper, for which CTE=1.7e-5, will shift the resonator frequency by that fraction of the resonator width, which would be, at best, somewhat beyond being acceptable. Tungsten or molybdenum would be greatly superior to copper in this respect. Acquiring and handling fragile tungsten split-cylinders is likely to be difficult and expensive. Molydenum would probably be preferale but, for now, we stick with copper.

This suggests the resonator dimensions should be constrained. It is sensible to leave the length unconstrained though, both because it would be difficult and because it is unnecessary—the increase in capacity is cancelled by the decrease in inductance. If the radius r_c is unconstrained, the inductance is proportional to r_c^2—doubling the effective expansion coefficient. More serious, though, would be the alteration of the gap spacing g_c. This suggests a design shown in the figure, with the gap width constrained by a dielectric with judiciously chosen temperature dependence of permittivity at the design frequency. Also shown in the figure are two tentative frequency tuning possibilities.

References

[1] Storage Ring EDM Collaboration, *A Proposal to Measure the Proton Electric Dipole Moment with* 10^{-29} *e-cm Sensitivity,* October, 2011

[2] J. Jackson, *Classical Electrodynamics,* 3rd edition, John Wiley, 1998

[3] W. Smythe, *Static and dynamic electricity,* 2nd edition, McGraw Hill, 1950

[4] V. Kumar, *Understanding the focusing of charged particle beams in a solenoid magnetic field,* Am. J. Phys. **77** (8) 2009

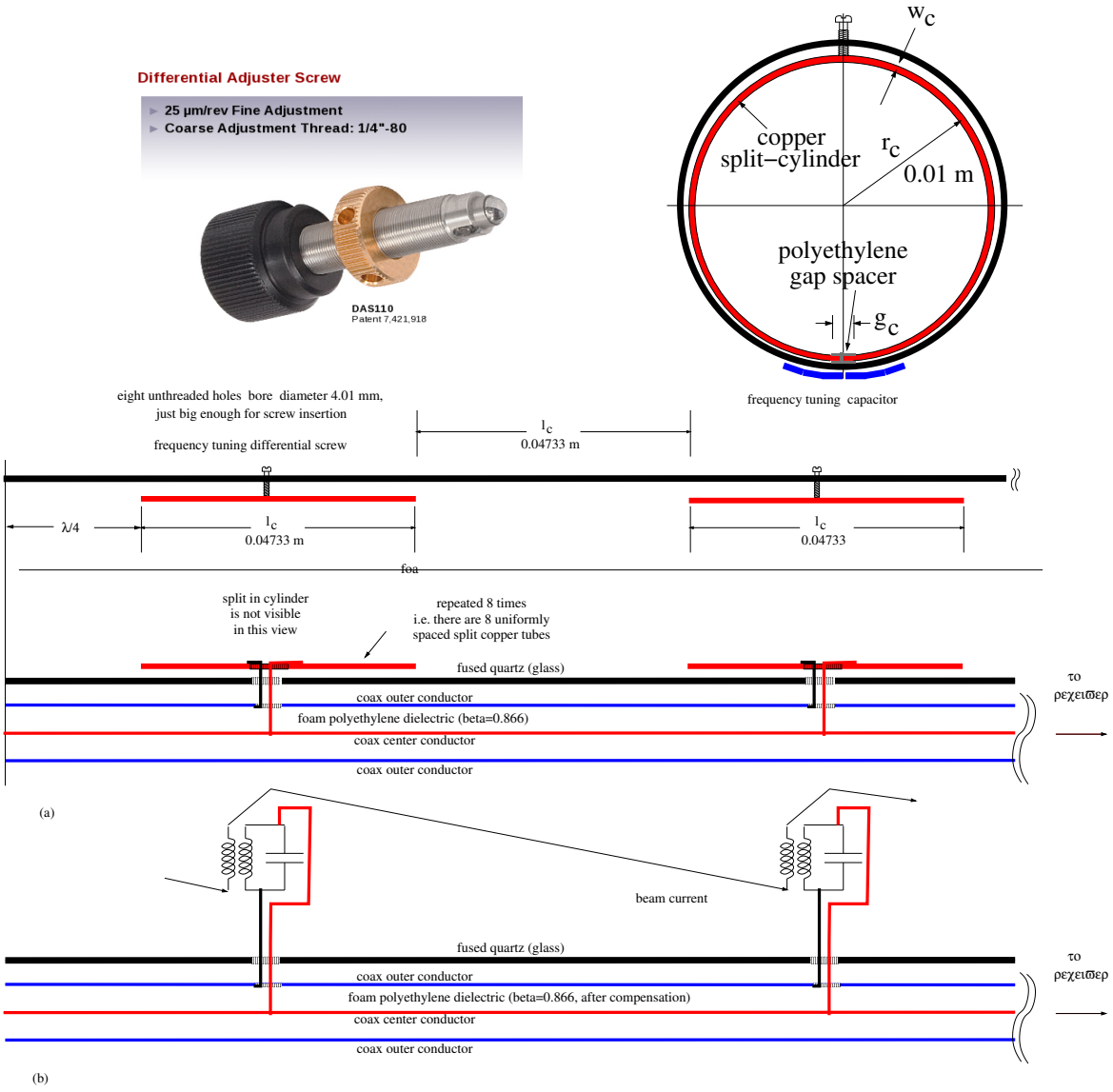

Figure 11: (a) Schematic of multi-element $h_c = 11$ split-cylinder electron polarimeter, with "end-fire" serial, coaxial readout. The signal velocity along the cable is equal to the beam velocity. Impedance matching (along with constructive interference of reflection from open circuit at the end of the transmission line remains to be confirmed. Parameters given in Table 1 apply only approximately to this figure. (b) Equivalent circuit representation.

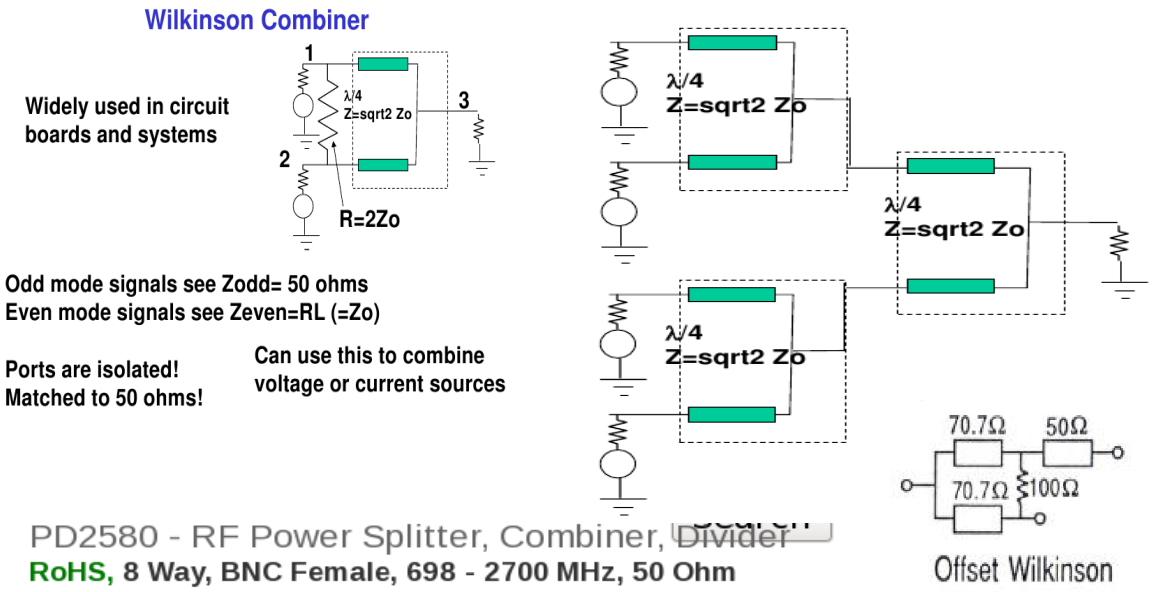

8 way Wilkinson RoHS power splitter combiner provides optimum broadband RF performance

- Wideband Frequency (698 - 2700 MHz)
- Low Insertion Loss (0.6 dB avg)
- High Port to Port Isolation (30 dB avg)
- Excellent VSWR (1.15 : 1 avg)
- RoHS Compliant Splitter Construction

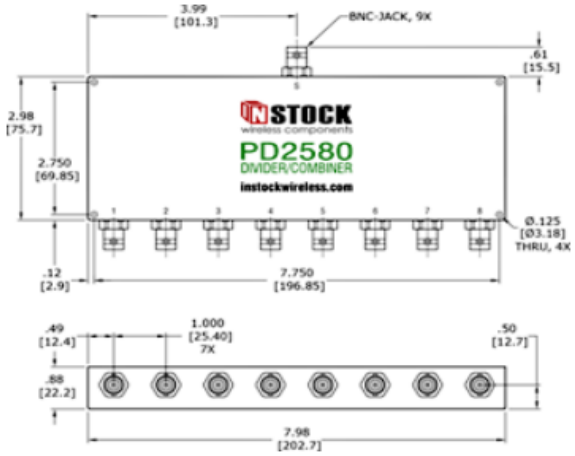

8-way power divider, power combiner with BNC Female coaxial connectors

Figure 12: Circuit possibilities for constructively adding the signals from multiple resonators. Timing will, of course, be critical. This requires the offset Wilkenson option, since each channel requires its own cable delay. What simplifies the summing is that all signals to be added are, in principle, identical. For maximal constructive interference, and to exploit the identical signal combining requirement, the channels have to be appropriately delayed to assure that the signals on all channels are synchronized in time. The 1 inch receiver input connector spacings for the signal combiner in the lower right would be about 1/4 of of the signal output terminal spacings for the $h_c = 11$ multi-element frequency option. This is of no particular significance; it is only to lend concreteness to the physical dimensions of the apparatus.

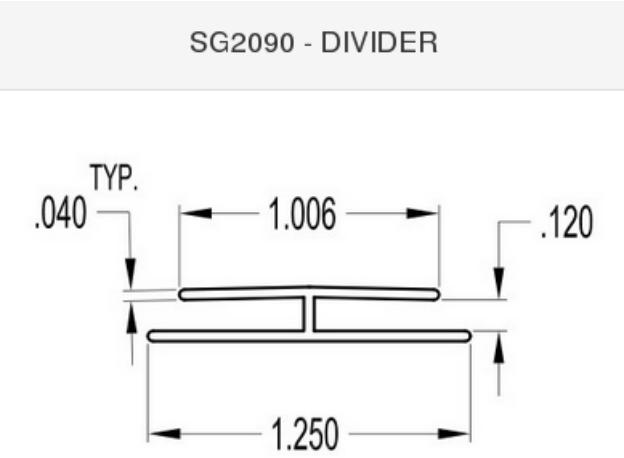

Figure 13: Extruded polyethylene gap separator. The dimensions are in inches. Relative permittivity=$\kappa_e = 2.4$. Loss tangent at 1 GHz=$\tan\delta < 5 \times 10^{-4}$. Coefficient of thermal expansion $= 1.30 \times 10^{-4}/^\circ$ C.